Agricultural and Forest Meteorology 200 (2015) 78–91

Contents lists available at ScienceDirect

Agricultural and Forest Meteorology

journal homepage: www.elsevier.com/locate/agrformet

Persistence of MODIS evapotranspiration impacts from mountain pine beetle outbreaks in lodgepole pine forests, south-central Rocky Mountains

Melanie K. Vanderhoof*, Christopher A. Williams

Graduate School of Geography, Clark University, 950 Main Street, Worcester, MA 01610, United States

ARTICLE INFO

Article history:
Received 6 May 2014
Received in revised form 6 September 2014
Accepted 21 September 2014

Keywords:
Evapotranspiration
Water cycle
Bark beetles
Mountain pine beetles
Disturbance
MODIS

ABSTRACT

The current extent and high severity (percent tree mortality) of mountain pine beetle outbreaks across western North America has been attributed to regional climate change, specifically warmer summer and winter temperatures and drier summers. This study paired multiple mountain pine beetle outbreak location datasets, both current and historical, with Moderate Resolution Imaging Spectroradiometer (MODIS) and Global Modeling and Assimilation Office (GMAO) Modern Era Retrospective-Analysis for Research and Applications (MERRA) products in order to quantify the full seasonal evapotranspiration impact of outbreak events for decades after outbreak (0 to 60 years). Following mountain pine beetle outbreaks in lodgepole pine (*Pinus contorta*) stands in the Colorado Rockies we observed an $18.7 \pm 1.4\%$ ($p < 0.01$) reduction in the rate of summer evapotranspiration at 14 to 20 years since outbreak. We also observed a $21.6 \pm 2.2\%$ ($p < 0.01$) increase in the rate of summer evapotranspiration, relative to non-attacked stands, in intermediate-aged stands 30 to 40 years since outbreak. Changes to growing season evapotranspiration correlated positively with changes in stand density, stand leaf area index (LAI) and the fraction of absorbed photosynthetically active radiation (fPAR), while high incoming solar radiation during the summer months acted to amplify changes to evapotranspiration even given relatively minor changes to summer fPAR and LAI due to the rapid regeneration of understory vegetation. Lodgepole pine mortality from mountain pine beetle outbreaks showed lasting effects on stand-scale evapotranspiration which could have important implications for regional water resources.

1. Introduction

The current extent and high severity (percent tree mortality) of recent bark beetle (Coleoptera: Curculionidae, Scolytinae) outbreaks across western North America is seen as a consequence of warmer summer and winter temperatures and drought conditions associated with regional climate change (Berg et al., 2006; Raffa et al., 2008). Warmer temperatures and drier conditions have reduced winter die-backs of bark beetle populations, increased the rate of bark beetle reproduction and maturation, and increased tree stress (Berg et al., 2006; Raffa et al., 2008). As a result, from 1997 to 2011, bark beetles have affected more than 41.7 million acres in the western United States and more than 6.6 million acres in Colorado alone, where mountain pine beetles (*Dendroctonus ponderosae*) have reduced the live basal area of lodgepole pine (*Pinus contorta*) dominated forests by 70%, on average (Klutsch et al., 2009; United States Forest Service (USFS), 2011). We can expect that such a mortality event, will, in turn, affect surface-atmosphere exchanges of water and energy (Bonan, 2008; Maness et al., 2012; Vanderhoof et al., 2014). Because of the large spatial extent and severity of mountain pine beetle attacks in forests across western North America, the impacts of these disturbance events and successive forest regeneration on the water balance needs to be both described and reliably predicted. The partitioning of precipitation into evapotranspiration, stream flow and water storage can vary widely in space and time in response to climate as well as changes to catchment vegetation. As evapotranspiration is a key component of both the water and energy cycles, a change in the evapotranspiration component can directly result in altered stream flow (Likens et al., 1994), surface temperatures (Wiedinmyer et al., 2012), and cloudiness (Bala et al., 2007).

The water cycle response to forest disturbance has been most extensively examined as post-harvest streamflow. An abundance

* Corresponding author. Present address: ORISE/U.S. EPA, Office of Research and Development, National Center for Environmental Assessment, 1200 Pennsylvania Ave., NW (8623-P), Washington, DC 20460, United States. Tel.: +1 703 347 0438; fax: +1 508 793 8881.
E-mail address: vanderhoof.melanie@epa.gov (M.K. Vanderhoof).

http://dx.doi.org/10.1016/j.agrformet.2014.09.015
0168-1923/

of studies have documented short-term increases in stream flow post-harvest, presumably from decreased transpiration (Bosch and Hewlett, 1982; Likens et al., 1994; Jones and Post, 2004). A reduction in water yield with afforestation or reforestation has also been observed (Swift and Swank, 1981; Scott and Smith, 1997; Jones and Post, 2004), and found to peak in intermediate aged stands (Shiklomanov and Krestovsky, 1988; Jones and Post, 2004). However, both the persistence of changes in streamflow as well as the directionality of the change has been found to be highly variable depending on stand species composition (Jones and Post, 2004; Moore et al., 2004), water table depth (Constantin et al., 1999), topography and aspect (Bonan, 2008; Barker et al., 2009), and climate (Farley et al., 2005).

When evapotranspiration components are directly measured, patterns can be even less consistent. A reduction in canopy cover following a disturbance can be expected to decrease overstory transpiration and interception, but it can also increase surface wind and solar energy which can elevate bare soil evaporation (Wilson et al., 2000; Gholz and Clark, 2002) as well as the transpiration of understory vegetation (Adams et al., 2012). Because of this, studies show mixed findings regarding rates of evapotranspiration and stand age (Gholz and Clark, 2002; Amiro et al., 2006; Jassal et al., 2009; Clark et al., 2012). In addition, unlike harvest events, standing snags following a mountain pine beetle attack will provide some shade for approximately 15 years post-outbreak, which will reduce the solar energy that reaches the ground (Griesbauer and Green, 2006). However, the remaining live trees following an attack typically experience an increase in productivity, and presumably transpiration, due to the increase in available resources (e.g. light, water, nutrients), which may partially compensate for the reduction in vegetation cover (Messier et al., 1999; McCarthy, 2001; Brown et al., 2014). The complex relationship between stand growth, soil evaporation, transpiration, and interception patterns makes it difficult to predict the temporal recovery of actual evapotranspiration following a disturbance event (Naranjo et al., 2012).

Several recent studies have quantified the evapotranspiration impacts in the years immediately following mountain pine beetle outbreaks. Reductions in evapotranspiration have been documented by both Maness et al. (2012) (19% reduction in summertime evapotranspiration) and Bright et al. (2013) (13–44% reduction in summer evapotranspiration, depending on outbreak severity) using the Moderate Resolution Imaging Spectroradiometer (MODIS) evapotranspiration product, however in contrast, Brown et al. (2014), using the eddy covariance technique, found understory transpiration and soil evaporation compensated for loss of overstory vegetation following even severe outbreaks. This was further supported by the finding that, unlike nearby clearcut sites, mountain pine beetle attacked forests were growing season carbon sinks due to the vigorous growth of remaining live trees (Brown et al., 2010). Most of the studies following mountain pine beetle outbreaks have quantified the impacts of other parts of the hydrological cycle, including stream flow and snow pack accumulation and melt. Several studies have documented increases in water yield following outbreaks (Potts, 1984; Bethlahmy, 1974). Correspondingly, Mikkelson et al. (2013) used hydrological models to predict that outbreaks would decrease evapotranspiration, increase snow accumulation, cause an earlier and faster snowmelt, and increase runoff volume and timing. Winter and spring findings have been confirmed by multiple field plot studies which have found higher snow pack accumulation during the gray attack phase, particularly in low to average snowfall years, and earlier snowmelt in both red and gray attack stages, due most likely to a reduction in albedo with needle fall on snow during the red-attack phase, and to increased canopy shortwave transmission during the gray-attack phase (Bewley et al., 2010; Boon, 2012; Pugh and Small, 2012). During the growing season, Clow et al. (2011) documented a localized increase in soil moisture beneath trees killed by mountain pine beetles, indicating a potential reduction in evapotranspiration.

Despite the widespread extent of current mountain pine beetle outbreaks, very few studies have directly quantified the impact of these mortality events on forest evapotranspiration, particularly post-gray attack stage (i.e. during snag fall and forest recovery). Patterns of evapotranspiration following harvest can inform expected patterns following mountain pine beetle outbreaks, however, differences between the disturbance types, such as soil compaction, snag or bole removal, and pattern and timing of mortality, limits the applicability of some of these associated findings. Our study pairs historical and current mountain pine beetle outbreak data with satellite data, within the Colorado Rockies. We aim to (1) quantify the seasonal patterns of change to evapotranspiration from attack start through 60 years post-attack, and (2) explore the meteorological and vegetation mechanisms that explain the evapotranspiration response. Changes to evapotranspiration and streamflow are especially critical in Colorado, as the Colorado Rockies provides the headwaters for several major rivers including the Colorado River, the Rio Grande, the Arkansas River and the Platte River.

2. Methods

2.1. Study area

Mountain pine beetle attacked and non-attacked sites were restricted to lodgepole pine dominated forests within the Colorado Rocky Mountains (Fig. 1). Lodgepole pine is found throughout the western United States and northwestern Canada on the lower slopes and valleys above the foothills at elevations between 2100 and 2900 m. The species occurs in both pure stands as well as in mixed stands. Common co-occurring tree species include aspen (*Populus tremuloides*), Douglas fir (*Pseudotsuga menziesii*), Engelmann spruce (*Picea engelmannii*) and subalpine fir (*Abies lasiocarpa*). Based on climatological records from Estes Park, CO (2365 m elevation) the average low and high temperature is −9 °C in January and 25 °C in July, respectively. Annual precipitation, derived from eight meteorological stations near the study sites, averages 521 to 1076 mm yr^{-1} (1910–2010). In comparison annual precipitation in 2011 and 2012 across the study area, as derived from the monthly Tropical Rainfall Measuring Mission Project (TRMM) precipitation dataset (Kummerow et al., 1998), was 435 ± 51 mm yr^{-1} and 296 ± 57 mm yr^{-1}, respectively. Precipitation data was not available for most months in 2011 and 2012 for seven of the eight meteorological stations, and the TRMM precipitation dataset was only available from 1998 to present necessitating the mixing of precipitation sources. In Rocky Mountain lodgepole pine stands, two-thirds of the annual precipitation typically occurs as snow, resulting in a hydrological cycle driven by snowmelt (Fahey and Knight, 1986).

2.2. Data descriptions

Early attempts to calculate evapotranspiration from remotely sensed data relied on the energy flux approach, in which evapotranspiration was calculated as the residual of available energy (net radiation − ground heat flux − sensible heat flux = evapotranspiration) (Kustas and Norman, 1999; Bastiaanssen et al., 1998; Allen et al., 2005). However, accurate estimation of the sensible heat flux, and in particular, the near-surface vertical air temperature difference, a component of the sensible heat flux, is consistently regarded as a problematic aspect of this approach (Bastiaanssen et al., 1998; Cleugh et al., 2007), particularly over forests where this temperature gradient is very small, due to high surface roughness (Nishida et al., 2003). Because of this,

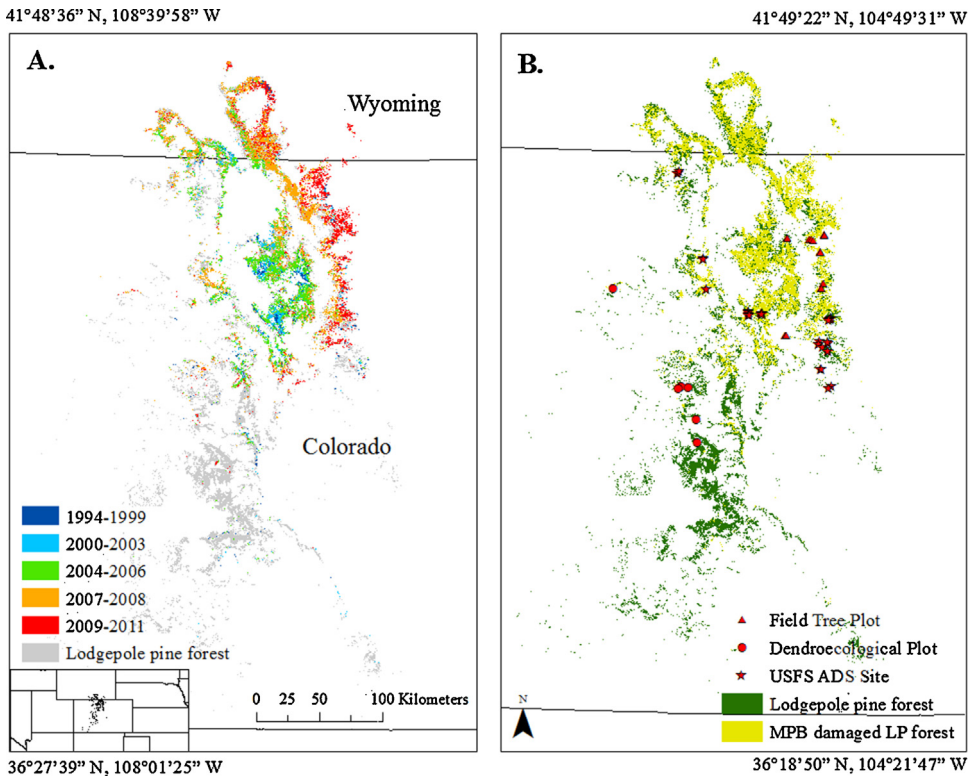

Fig. 1. (A) Progression of mountain pine beetle outbreaks over the last two decades within lodgepole pine stands in Colorado and southern Wyoming. (B) Plot locations for field tree plots, dendroecological plots and U.S. Forest Service (USFS) aerial detection survey (ADS) sites. MPB refers to mountain pine beetle, while LP refers to lodgepole pine.

the MOD16A2 Collection 5 global evapotranspiration dataset (Mu et al., 2011) was used as the primary means of calculating evapotranspiration because it relies on the Penman–Monteith equation (Monteith, 1965), which directly calculates evapotranspiration. In addition, this product has been successful in other applications to quantify the evapotranspiration impacts of mountain pine beetle outbreaks (Maness et al., 2012; Bright et al., 2013). This product is provided at 1 km^2 at 8-day intervals. The MOD16A2 evapotranspiration dataset calculates evapotranspiration as the sum of evaporation from wet and moist soil, interception, and transpiration (Mu et al., 2007, 2011). Stomatal conductance is specified by biome specific vapor pressure deficit and daily minimum temperature thresholds, while the leaf area index is used to scale stomatal conductance to canopy conductance. The product showed seasonal patterns of evapotranspiration consistent with expectations, so we have included winter evapotranspiration results; however, the MODIS product algorithm makes no adjustments to account for the presence/absence of snow cover and assumes that bare soil evaporation is sufficient to calculate winter snow melt and subsequent evaporation as well as snow sublimation. This assumption is problematic and should be revised in future versions of the algorithm. Within this analysis winter evapotranspiration results should be interpreted with caution. Details regarding how the algorithm responded to our data during the winter months are provided in Appendix A.

MODIS data inputs into the Collection 5 MOD16A2 evapotranspiration algorithm include 1) global Collection 4 annual land cover type 2 at 500 m^2 resolution (MCD12Q1) (Friedl et al., 2002); 2) Collection 5 8-day leaf area index—FPAR at 1 km^2 resolution (MOD15A2) (Myneni et al., 2002); and 3) Collection 4 0.05-degree 16-day CMG MODIS albedo (the 10th band of the White-Sky-Albedo from MOD43C1) (Jin et al., 2003; Schaaf et al., 2002). NASA's Global Modeling and Assimilation Office (GMAO) Modern-era retrospective analysis for research and applications (MERRA) Goddard Earth Observing System Data Assimilation System Version 5 (GEOS-5) daily meteorological reanalysis data (1.00 × 1.25°) for air temperature (°C), actual vapor pressure (Pa), relative humidity (fraction) and incoming solar radiation (W m^{-2}) are also used as inputs. The MOD16A2 data utilized was limited to 2012, in order to minimize differences between the satellite spectral information and field observations (collected in the summer of 2012). However, because 2012 experienced lower than normal precipitation, data from 2011 were also analyzed. To capture seasonal evapotranspiration variation, we examined all 92 dates available between January 1, 2011 and December 31, 2012. Within each image, we rejected pixels classified as problematic (QC = 97, 105 or 113) or fill (QC = 157). Only pixel values spatially concurrent with field locations were used.

Data on locations of mountain pine beetle outbreaks were derived from three sources: (1) field data on tree attributes collected in plots (39 sites), (2) historic U.S. Forest Service Aerial Detection Surveys (ADS) (33 sites), and (3) field-based dendroecological plots (6 sites) (Table 1, Fig. 1). Using the global Collection 4 land cover type 2 (MOD12Q1), only plot locations classified as evergreen needleleaf forest by the International Geosphere–Biosphere Programme and University of Maryland cover types were included in the analysis. Further, the MODIS pixel extent for each field plot was reviewed using 2011 National Agriculture Imagery Program (NAIP) imagery to check for consistency of forest cover and damage patterns. Plots within

MODIS pixels that were <75% coniferous forest cover were removed from the analysis. Field-collected tree plot data were collected in lodgepole pine dominated stands from 18 June to 20 July 2012, within 900 m^2 plots (35,100 m^2 total). Plots were targeted to be representative of (1) the surrounding 500 m × 500 m area, (2) a severity spectrum (from none to severe) of mountain pine beetle outbreak, and (3) a spectrum of time since attack (green attack, red attack and gray attack stages). Plots were on average 93% lodgepole pine. Within each plot, each tree was identified to the species level,

Table 1
The number and source of mountain pine beetle outbreak locations and pixels utilized by time interval or time since mountain pine beetle outbreak.

Time interval	Number of sites/source	Number of sites/source	Total no.	Total no. of MODIS ET pixels
1–3 Years	7/2012 Tree plots		7	184
4–13 Years	15/2012 Tree plots		15	671
14–20 Years	3/2012 Tree plots	14/USFS ADS sites	17	690
21–30 Years	5/2009 Dendro plots	5/USFS ADS sites	10	458
31–40 Years	1/2008 Dendro plot	9/USFS ADS sites	10	456
50–60 Years	5/USFS ADS sites		5	229
		Total	64	2688

its diameter at breast height (dbh) measured (dbh >7.5 cm), and recorded as un-attacked (no evidence of beetle presence), green attack stage (exit holes and pitch tubes present but needles still green), red attack stage (exit holes and pitch tubes present and needles red) or gray attack stage (exit holes and pitch tubes present and needles absent), or unknown dead (needles absent, but no evidence of beetle damage). Plots were categorized by attack stage (healthy, red, gray), where attacked plots were categorized as red if the majority of attacked trees were in the red attack stage, or gray if the majority of the attacked trees were in the gray attack stage. Within plots classified as "attacked" the percent dead trees ranged from 16% to 81% with a mean percent tree mortality of 50%.

The primary source for historic (>16 years since outbreak) mountain pine beetle outbreak locations was geo-referenced U.S. Forest Service Region 2 Aerial Detection Survey (USFS ADS) maps (1956–1987). These maps were periodically created by expert surveyors to record "new damage" polygons during flown surveys. Although an absence of a polygon does not necessarily indicate true absence due to the incomplete spatial nature of these surveys, a drawn polygon provides high confidence of the presence of an outbreak. To reduce potential error regarding the location of these outbreaks, historic outbreak plot locations were located at the center of "damage" polygons larger than a MODIS pixel. Additionally, polygons of historic outbreaks were eliminated from consideration if they (1) overlapped with damage polygons identified in later USFS Region 2 ADS maps (1994–2011) or (2) overlapped with the locations of past fires (1984–2011) as derived from Monitoring Trends in Burn Severity (MTBS) data (Eidenshink et al., 2007). In addition, a disproportionate number of downed trees, relative to a typical mature forest, were observed using aerial imagery within most historic damage locations, corroborating past outbreaks.

Additional historic mountain pine beetle outbreaks were located using dendroecological methods that have been previously tested (Heath and Alfaro, 1990; Alfaro et al., 2010) and applied (Axelson et al., 2009; Kulakowski and Jarvis, 2011; Kulakowski et al., 2012) to lodgepole pine stands to reconstruct stand disturbance history in this and other regions. Lodgepole pine-dominated sites were randomly selected for dendroecological reconstruction of mountain pine beetle outbreaks (Kulakowski et al., 2012; Dan Jarvis, personal communication). In each stand increment cores were collected from living host and non-host and dead host trees. These cores were used to derive dates of stand-origin, tree mortality and releases (abrupt two-fold increases in ring width sustained for more than 10 years). Additional methodological details are provided in Kulakowski et al. (2012). Data were collected in summer of 2008 (Kulakowski et al., 2012) and summer of 2009 (Dan Jarvis, personal communication).

2.3. Analysis

Mountain pine beetles have predominately moved from west to east across the Colorado Rocky Mountains over the past several decades (Fig. 1). This outbreak dynamic necessitated a minimum study area size in order to include outbreak locations from a wide range of outbreak ages. However, the size of the study area, in turn, resulted in the potential for inherent spatial variability in evapotranspiration values due to variation in climate parameters which can change rapidly throughout a mountainous region. To correct for this potential bias, evapotranspiration with time since mountain pine beetle outbreak was calculated as the within scene change in evapotranspiration from "local" non-attacked forest. Non-attacked forest polygons were defined as lodgepole pine forest that was not identified as attacked by USFS ADS surveys (1994–2011) or MTBS data (1984–2011). We also used the MODIS-derived LAI values of field-based non-attacked tree plots to set seasonally specific lower and upper LAI limits for potential non-attacked forest locations. Non-attacked forest points (196 total points) were randomly selected from the center of these identified polygons. "Local" non-attacked forest evapotranspiration was then calculated as the mean evapotranspiration for "local" non-attacked forest locations. "Local" was defined as occurring primarily within 20 km and no more than 50 km from each individual attacked plot location. We averaged 19 non-attacked forest locations per attacked plot. We further normalized these results by calculating change as the percent change in evapotranspiration (ET) from the within scene local non-attacked forest ((attacked forest ET − non-attacked forest ET)/(non-attacked forest ET) × 100). Percent change in evapotranspiration was then averaged by time intervals to derive change in evapotranspiration with years since outbreak start. Time intervals were defined as: 1–3, 4–13, 14–20, 21–30, 31–40, and 50–60 years since disturbance. The width of the time intervals was based on our confidence in deriving an accurate year of outbreak. The time intervals of 41–50 and >60 years since mountain pine beetle outbreak were not included due to small sample sizes.

The change in MODIS evapotranspiration input parameters (LAI and fPAR (MOD15A2) and 0.05-degree CMG MODIS albedo (MOD43C1)) with time since attack start were also tested. In contrast to climate parameters, stand structure tends to be fairly homogenous across lodgepole pine forests within Colorado. Percent change to LAI, fPAR and albedo with years since outbreak were derived by comparing attacked plots to field-based non-attacked tree plots. We also calculated percent change to LAI, fPAR and albedo using local non-attacked forest, but found the magnitude and patterns of change to be similar regardless of the method used.

Using the algorithm specified primarily in Mu et al. (2011) and secondarily in Mu et al. (2007) we tested the sensitivity of monthly evapotranspiration to changes in input parameters. The results of the sensitivity analysis were specific to our study area and time period. Elevation was derived from a 50 m resolution digital elevation model (DEM) and is used in the model algorithm to quantify atmospheric pressure. We calculated one-tailed 95% confidence intervals (calculated from variation between plots and within a given season) for all raw model input parameters (fPAR, LAI, albedo, elevation, incoming shortwave solar radiation, air temperature, relative humidity, and vapor pressure). We tested the effect of varying each parameter by plus and minus a fixed percentage (20%), which allowed us to compare the model sensitivity across parameters, as well as by the 95% confidence interval of each parameter, which

provided additional insight into the actual variability of the input parameters within our study area and time period. Finally, gray attack stage (14 to 20 years since outbreak) tree plot data was analyzed to quantify the change in evapotranspiration with outbreak severity and ground characteristics. Corresponding Pearson pair-wise correlations and paired *t*-tests were calculated using SPSS Statistics (IBM Corporation, Armonk, NY).

3. Results

3.1. Validation of MODIS evapotranspiration product

As a global product, the MODIS evapotranspiration product was not necessarily designed for application to local and regional research questions; therefore we must consider the potential error within the MODIS evapotranspiration product. The MODIS evapotranspiration algorithm relies on temperature, vapor pressure and humidity reanalysis data instead of precipitation data, so we validated the MODIS evapotranspiration product within our study area by independently calculating evapotranspiration within a watershed using a simplified version of the water balance equation ($ET = P - Q$), where P is precipitation and Q is run-off. Many streams with water gauge instrumentation within our study area are dammed and contain completely regulated flow, precluding their use for estimating evapotranspiration from a water balance equation. We used Bear Creek (USGS 06710385) in Jefferson County, Colorado which has a drainage area of 267 km^2. This watershed has natural flow, affected only by minor diversions for irrigation and contained eight of our historical outbreak plot locations. Annual evapotranspiration for 2011 and 2012 was estimated by subtracting annual stream flow from annual precipitation, as derived from the monthly TRMM precipitation dataset (TRMM Product 3B43) which has a spatial resolution of $0.25^\circ \times 0.25^\circ$ (Kummerow et al., 1998). Annual change in soil water storage was assumed to be minimal. These estimates were compared to MODIS evapotranspiration averaged annually, across the watershed area and showed acceptable agreement. In 2011 the estimate of evapotranspiration from the water balance equation was 21.9% higher than from the MODIS evapotranspiration product (400.3 mm yr^{-1} compared to 312.5 mm yr^{-1}), but in 2012, these two estimates were only 3% different (302.2 mm yr^{-1} compared to 293.2 mm yr^{-1}, respectively). Additional validation efforts at a broader spatial scale are shown in Mu et al. (2011).

3.2. Response of evapotranspiration with time since outbreak

The response of evapotranspiration with time since outbreak start was found to vary by season. Using the 2012 MODIS evapotranspiration dataset, changes to evapotranspiration, relative to non-attacked forests, peaked during the summer months. We observed an $18.7 \pm 1.4\%$ ($p < 0.01$) reduction in the rate of summer evapotranspiration, relative to non-attacked forests, at 14 to 20 years since outbreak (Fig. 2). This timing coincided with the typical peak in post-outbreak snag fall (Mitchell and Preisler, 1998). We also observed a $21.6 \pm 2.2\%$ ($p < 0.01$) increase in the rate of summer evapotranspiration, relative to non-attacked stands, in intermediate-aged stands 30 to 40 years since outbreak (Fig. 2). Winter months showed the opposite pattern as summer, with winter evapotranspiration peaking at 14 to 20 years since outbreak, with an increase of $14.9 \pm 1.0\%$ ($p < 0.01$), relative to non-attacked forests, followed by a $9.4 \pm 1.8\%$ ($p < 0.01$) reduction in evapotranspiration in intermediate-aged stands 30 to 40 years since outbreak. To ensure that this pattern was not restricted to 2012, we also tested change to evapotranspiration using all scenes from 2011. Despite 2012 being drier than 2011, seasonally specific patterns of change were very similar. When we focused on interannual differences within the summer months, the initial reduction in evapotranspiration following an outbreak was more consistent throughout the summer months in 2012 relative to 2011, however, both years showed the initial reduction in evapotranspiration peaking in June (Fig. 3). In addition, both years showed a similar sized peak in evapotranspiration coinciding with 30 to 40 years since outbreak (Fig. 3).

Examining patterns of change for key periods (14 to 20 years and 30 to 40 years since outbreak) over the course of the year, instead of seasonal averages, also helped confirm and explain patterns of change. The rates of evapotranspiration in both non-attacked and attacked forests peaked during the summer months (Fig. 4). Change to evapotranspiration for both intervals also peaked during the summer months, with plots 14 to 20 years since outbreak showing consistent reductions in evapotranspiration relative to non-attacked, and plots 30 to 40 years since outbreak showing consistent elevations in evapotranspiration (Fig. 4). A difference in the rate of evapotranspiration between the two local non-attacked forests demonstrated the importance of calculating change in evapotranspiration as a function of change from local non-attacked forest. In addition, we also calculated non-normalized, absolute change in seasonal and annual evapotranspiration with time since outbreak, which is included in Appendix A (Fig. A1). On an annual timescale, a muted version of the growing season pattern with time since outbreak persisted (Fig. A1).

3.3. Explaining MODIS ET patterns using model algorithm and product inputs

We utilized the MODIS evapotranspiration algorithm data inputs as well as the algorithm itself to explain both patterns with time since outbreak and differences in patterns between seasons. By calculating evapotranspiration as change from local non-attacked forest we controlled, to the extent possible, for change in evapotranspiration caused by spatial variation in climate parameters. Consequently, derived patterns in evapotranspiration with time since outbreak are primarily the result of changes to non-climate MODIS product inputs (fPAR, LAI and albedo). The parameter fPAR is used in the algorithm to define the fraction vegetation versus bare soil, and therefore heavily influences the quantified rate of plant transpiration and evaporation from bare soil within the algorithm. LAI is used to calculate several resistance parameters including surface resistance to plant transpiration, wet canopy resistance, and wet canopy resistance to sensible heat, while albedo influences net radiation (Mu et al., 2011). A seasonally specific sensitivity analysis of the evapotranspiration model showed that the model was highly sensitive to changes in vegetation amount, specifically fPAR and LAI, in the growing season, but less sensitive to changes in albedo, while in the winter months the model was highly sensitive to changes in fPAR, but less sensitive to changes in LAI or albedo (Fig. 5). Change in fPAR, LAI and albedo with years since outbreak start are shown in Fig. 6. Patterns of change to fPAR, LAI and albedo, all indicators of vegetation amount and condition, correlated positively with changes to growing season evapotranspiration. Change to vegetation was largest in the winter months, likely due to seasonal leaf loss and snow which masks possible contributions from the regeneration of understory vegetation post-outbreak. Following an outbreak, the decrease in fPAR and LAI peaked in winter months at 14 to 20 years with a $42.6 \pm 3.2\%$ and $45.6.5 \pm 3.5\%$ reduction, relative to local non-attacked forests, respectively (Fig. 6). Additionally we observed a peak in fPAR and LAI at 30 to 40 years post-outbreak with a winter increase in fPAR and LAI of $31.3 \pm 3.0\%$ and $49.1 \pm 4.6\%$, relative to non-attacked forests, respectively. Within the modeled product, a large decrease in fPAR in the winter months following

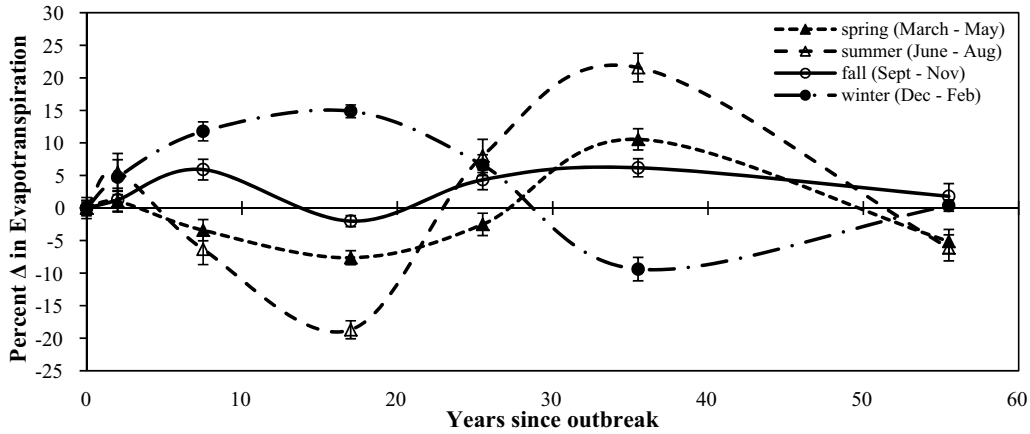

Fig. 2. Percent change in seasonal evapotranspiration with years since outbreak for 2012. Change is calculated relative to local, for each plot, non-attacked forest. Error bars are plus and minus standard error.

mountain pine beetle outbreaks resulted in a higher fraction "bare ground" which increased the relative importance of the modeled soil evaporation component during cold months in which the rate of transpiration was minimal. This helped to explain why winter evapotranspiration showed an inverse relationship with vegetation amount following mountain pine beetle outbreaks. Additional details are provided in Appendix A. In contrast, the growing season evapotranspiration model was highly sensitive to changes in fPAR and LAI and both of these indices were highly positively correlated with the changes in the modeled evapotranspiration. Additionally, when key intervals were examined over the course of the year, a reduction to summer evapotranspiration at 14 to 20 years post-outbreak was coincident with a lower fPAR and LAI, while an elevation in the rate of evapotranspiration at 30 to 40 years post-outbreak was coincident with higher fPAR and LAI (Fig. 4)

One observation we noted was that a relatively minor change in vegetation amount (fPAR, LAI) resulted in an unexpectedly larger decrease in summer evapotranspiration. For example a decrease of $9.4 \pm 0.8\%$ in summer fPAR at 14 to 20 years resulted in a reduction of $18.7 \pm 1.4\%$ in summer evapotranspiration. Although spatial variability in incoming shortwave radiation and temperature were controlled for in the analysis by calculating evapotranspiration as percent change from adjacent non-attacked forest, both

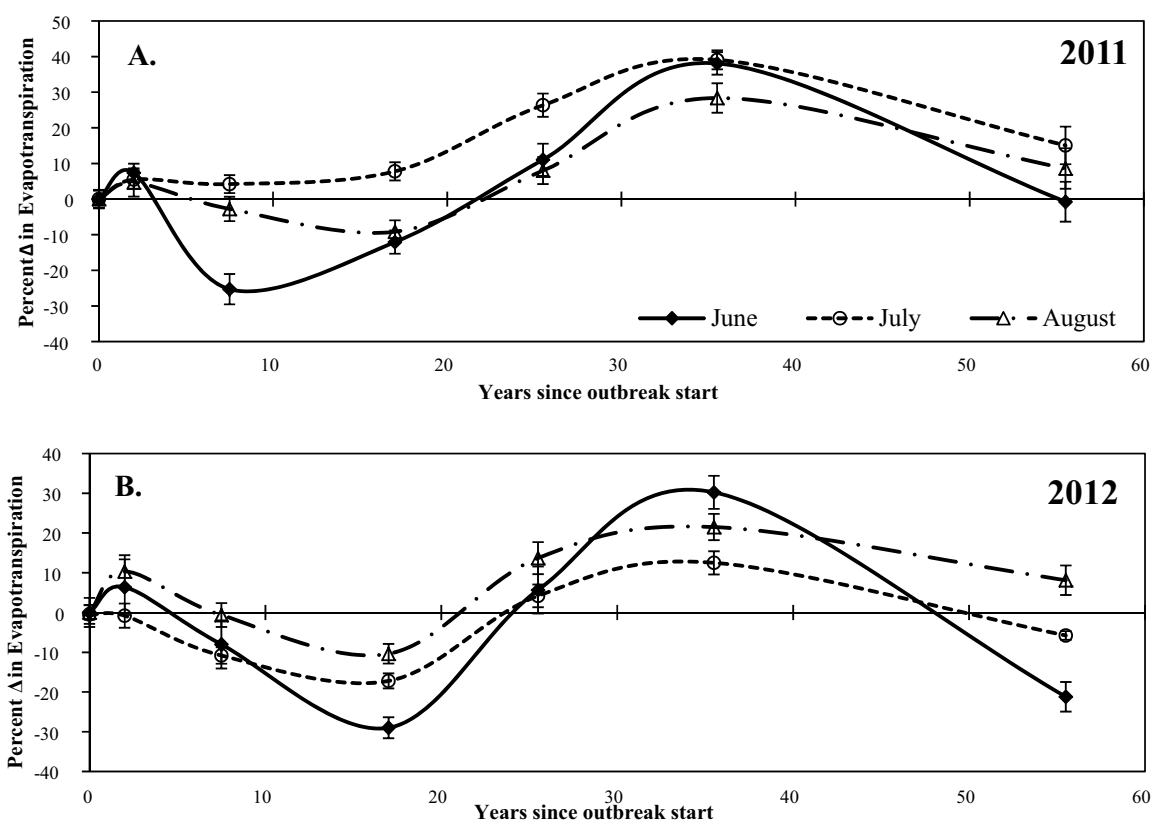

Fig. 3. Change in monthly evapotranspiration with years since outbreak start during the summer months of (A) 2011 and (B) 2012. Error bars represent plus and minus standard error.

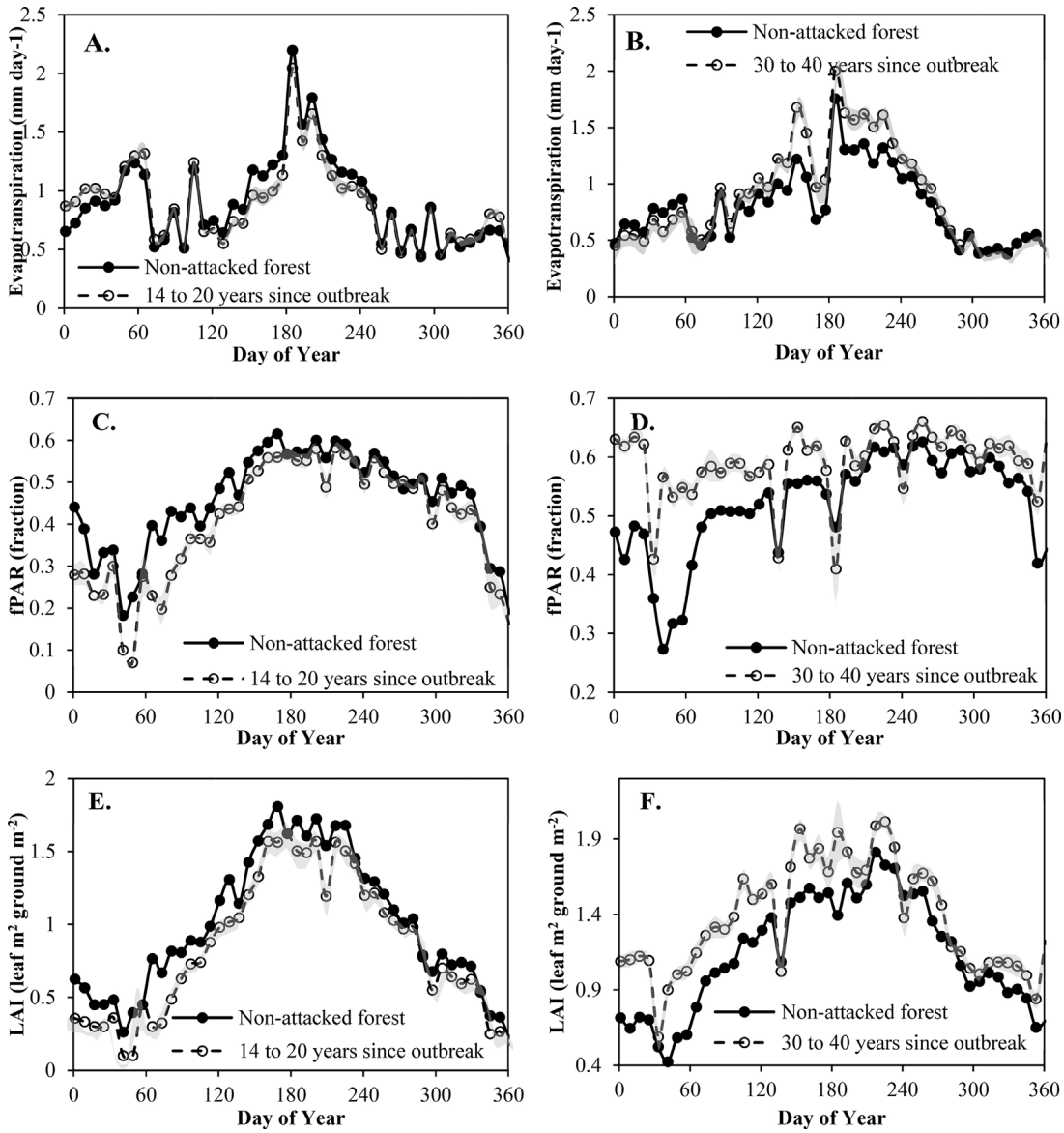

Fig. 4. Mean 2012 evapotranspiration for 8 day periods of local non-attacked forest, calculated as the average of non-attacked forest associated with each of the plots within the respective time intervals, relative to the average of attacked forest for (A) 14 to 20 years since outbreak and (B) 30 to 40 years since outbreak. Eight-day average for non-attacked forest, 14 to 20 years since outbreak and 30 to 40 years since outbreak of fPAR (C and D, respectively) and LAI (E and F, respectively). Shaded region shows plus and minus standard error for attacked forests.

parameters showed strong seasonal patterns (Fig. 7). It is possible that seasonal differences in incoming solar radiation and temperature may act to amplify or dampen the sensitivity of evapotranspiration to changes in fPAR and LAI. When changes in fPAR were graphed against changes in evapotranspiration as a function of air temperature and incoming shortwave radiation, we found that for incoming shortwave radiation, in particular, the change in evapotranspiration, given a change in fPAR was much larger under highdiurnal incoming solar radiation conditions (>350 W m^{-2} monthly mean) ($y = 1.11x + 47.86$, $R^2 = 0.49$, $p < 0.01$) relative to moderate diurnal incoming solar radiation conditions (215–350 W m^{-2} monthly mean) ($y = 0.23x + 13.22$, $R^2 = 0.09$, $p < 0.01$) or low diurnal incoming solar radiation conditions (<215 W m^{-2} monthly mean) ($y = -0.35x - 9.07$, $R^2 = 0.41$, $p < 0.01$). This significant interaction suggests that incoming solar radiation, in particular, may have acted to amplify the response of summer evapotranspiration to changes in fPAR and LAI, relative to other seasons.

3.4. Change in evapotranspiration with outbreak severity

In addition to exploring the change in evapotranspiration with time since outbreak, we can also hypothesize that the evapotranspiration response will vary with outbreak severity. Outbreak severity has been defined here as percent dead trees. For this measure of severity to be comparable between plots, however, starting stand density (live and dead trees) should be relatively similar. Although stand density showed a large range (666.67 trees per hectare to 3978 trees per hectare), over 70% of the plots showed a stand density between 900 and 2500 trees per hectare (mean stand density = 1829 ± 145 trees per hectare). Because of this variability, we have also considered the number of live trees remaining post-attack. We found a strong relationship between percent dead trees and the number of live trees per hectare when live trees were less than 2000 per hectare ($y = -0.043x + 79.29$, $R^2 = 0.81$), but that plots consistently exhibited much reduced mortality when the number of live trees was greater than 2000 live trees per hectare

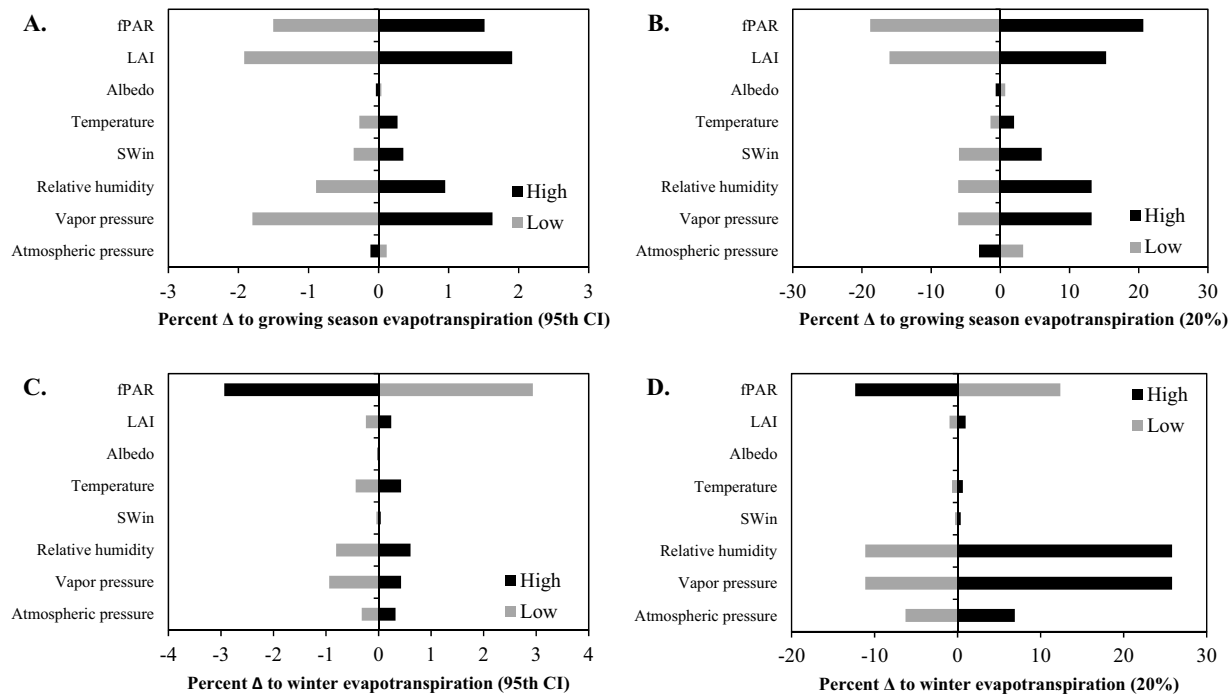

Fig. 5. Percent change in monthly MODIS evapotranspiration within the May to September growing season (panels A, B) or December to February winter season (panels C and D), each in response to plus or minus the 95th confidence interval of the MODIS evapotranspiration model input parameters (panels A and C), or a 20% increase or decrease in the MODIS evapotranspiration model input parameters (panels B and D).

(a threshold point). These plots likely represent young, dense stands which tend to be less targeted by mountain pine beetles compared to mature stands (Roe and Amman, 1970; Klutsch et al., 2009).

During the summer months (June–August) the rate of evapotranspiration decreased with fewer live trees per ha ($y = 0.0001x - 0.10$, $R^2 = 0.16$, $p < 0.01$) and a higher percent dead trees ($y = -0.34x + 13.73$, $R^2 = 0.22$, $p < 0.01$) (Fig. 8). During the snow-cover period evapotranspiration increased with increased percent tree mortality ($y = 0.27x - 3.32$, $R^2 = 0.47$, $p < 0.01$) and decreased with an increased number of live trees per hectare ($y = -0.00004x + 0.09$, $R^2 = 0.38$, $p < 0.01$) (Fig. 8). Although loss of tree canopy can be expected to decrease evaporation of intercepted snow, it can increase shortwave transmission and momentum of air to the surface, speeding the rate of snow sublimation or ablation (Musselman et al., 2008; Bewley et al., 2010; Pugh and Small, 2012), which is consistent with our winter findings albeit via the soil evaporation component of the MODIS ET algorithm. A decrease in the number of live trees post-disturbance can increase the importance of transpiration from saplings, seedlings and other understory vegetation (herbaceous vegetation and woody shrubs). The relative importance of this source of transpiration will depend on both the pre-attack density and post-attack response of understory vegetation and seedling/sapling abundance. During the gray attack stage, percent understory vegetation cover, for instance, increased strongly with increased percent dead trees ($y = 0.66x - 7.32$, $R = 0.72$, $p < 0.01$) and fewer live trees ($y = -0.013x + 35.36$, $R^2 = 0.38$, $p < 0.01$), suggesting that understory vegetation responds relatively rapidly to increased light availability post-attack. In addition, the percent understory vegetation was significantly related to the change in summer evapotranspiration ($R = -0.36$, $p < 0.05$) and winter evapotranspiration ($R = 0.48$, $p < 0.01$) (Table 2). In contrast, sapling/seedling density showed no significant relationship with percent dead trees or number of live trees. This finding suggests that seedling regeneration has not yet responded to the increased light availability at 4 to 13 years post-attack. Others have documented a suppression of new seedling establishment for the decade(s) following disturbance due to their competitive exclusion by understory trees and vegetation (Wickman et al., 1986; Wohlgemuth et al., 2002). Given that the percent understory vegetation increased with the percent dead trees, if understory vegetation was fully compensating for the dead trees during the snow-free period, then we should see no relationship between evapotranspiration and the percent dead trees. Although we still observed a significant relationship between percent tree mortality and evapotranspiration, we are unable to quantify how much, if any, the transpiration of understory vegetation is partially compensating for the dead trees.

4. Discussion

The primary contribution of this study is our examination of the change in evapotranspiration, not only immediately following a mountain pine beetle outbreak, but through 60 years post-disturbance. For context, lodgepole pine trees, where competition is limited, typically reach maturity (79 ft tall (24 m) and 16 inch (41 cm) in diameter) by 50 to 60 years (Amman, 1977) and we have documented a recovery in forest albedo by 30 to 40 years post-disturbance. Existing studies on the impacts of mountain pine beetle attacks on evapotranspiration, meanwhile, are limited to five years (Maness et al., 2012) and nine years (Bright et al., 2013) following attack start. We can, however, compare our findings during the initial period following attack. Bright et al. (2013) and Maness et al. (2012) both used seasonally averaged evapotranspiration (June–August) over an 11 year period. Maness et al. (2012) and Bright et al. (2013) documented a 19% or 13–44% decrease in summer evapotranspiration following a mountain pine beetle outbreak of 30% mortality on average or 10 to >50% mortality, respectively. In comparison, using a chronosequence approach, we documented only a 6.3 ± 2.4% reduction in summer evapotranspiration for 4 to 13 years post-attack, but an 18.7 ± 1.4% reduction in summer evapotranspiration from 14 to 20 years post-outbreak, with an average outbreak severity of 50% tree

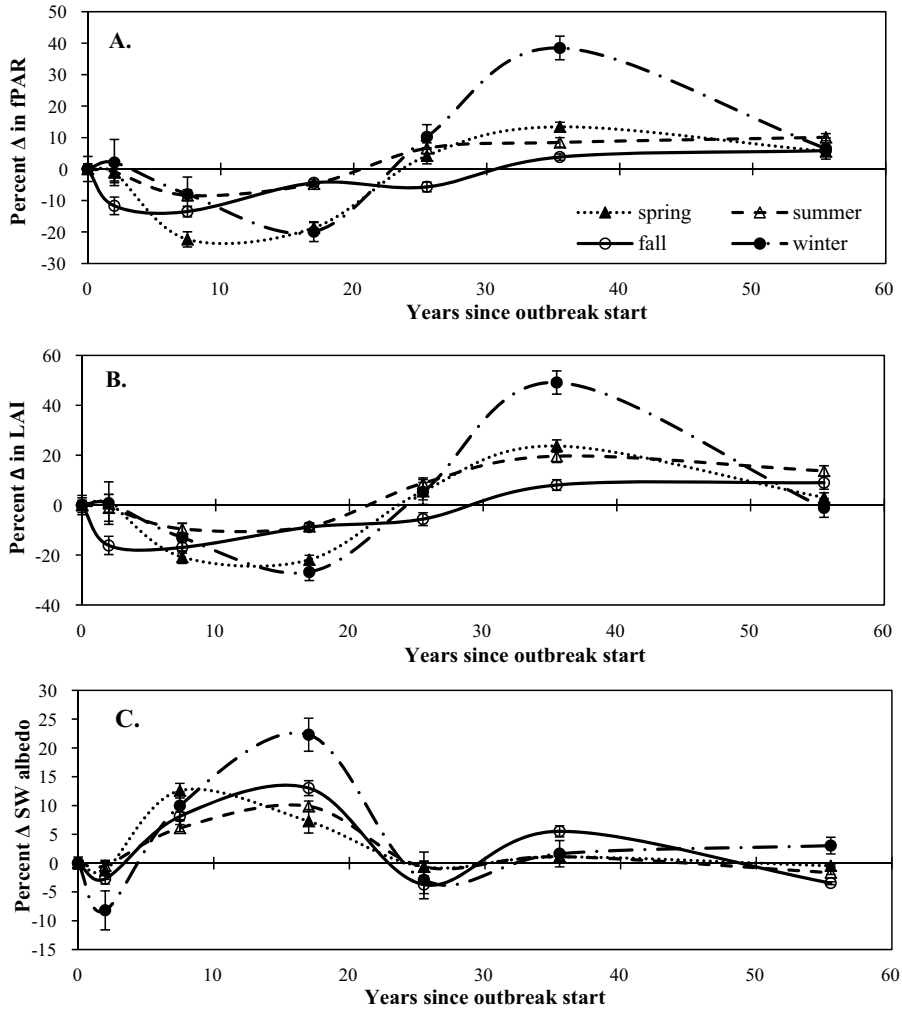

Fig. 6. Percent change with years since outbreak for (A) fPAR, (B) LAI and (C) shortwave broadband albedo.

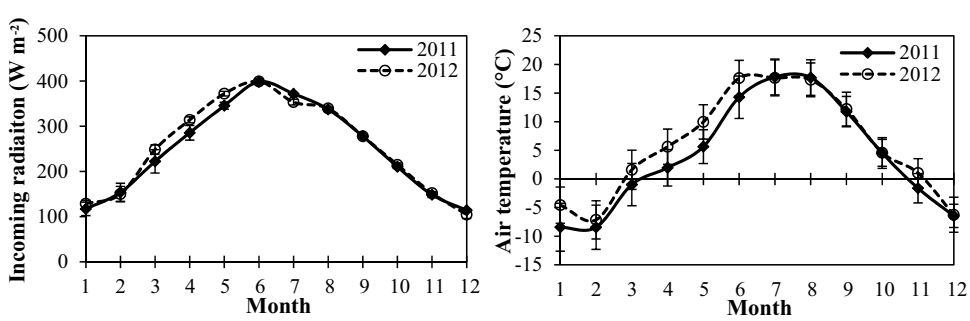

Fig. 7. Monthly averages of mean daily incoming shortwave radiation and air temperature averaged across the study area plots.

Table 2
Pearson correlation values between changes in evapotranspiration and stand characteristics within gray attack stage (4–13 years since attack) plots.

Season	% Dead trees	Living tree density	% Open sky visibility	% Understory vegetation	% Litter cover	Litter depth	% Rock cover	Sapling/seedlings per ha	Canopy height	Elevation	Slope
ΔET in Spring	−0.43**	0.43**	−0.28	−0.33*	0.35*	−0.10	0.05	−0.10	0.001	0.01	−0.05
ΔET in Summer	−0.48**	0.40**	0.19	−0.36*	0.33*	−0.20	0.07	−0.02	−0.19	−0.23	−0.18
ΔET in Fall	−0.27	0.16	0.11	−0.22	0.16	−0.28	0.16	−0.14	0.07	0.35*	0.04
ΔET in Winter	0.68**	−0.61**	0.53**	0.48**	−0.47**	−0.47*	−0.09	−0.23	0.39*	0.40**	−0.01

* Correlation is significant at the 0.05 level (1-tailed).
** Correlation is significant at the 0.01 level (1-tailed).

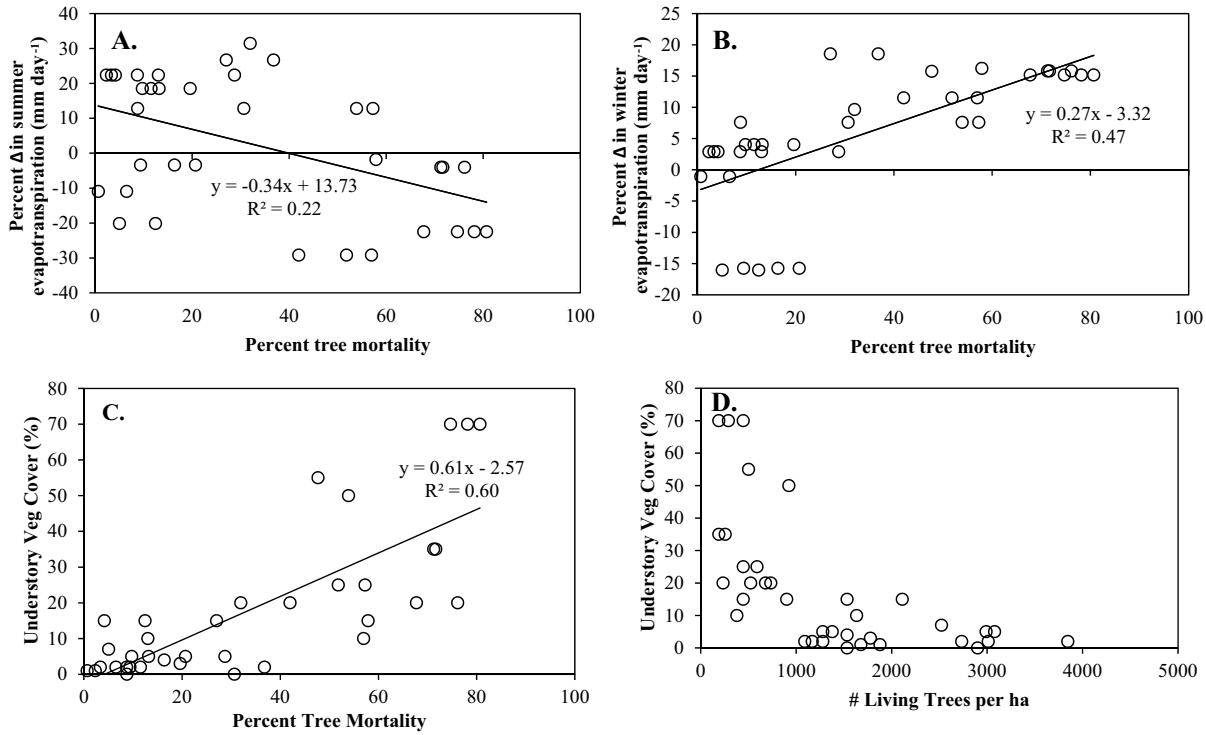

Fig. 8. (A) Change in summer evapotranspiration in relation to percent tree mortality during the gray attack stage. (B) Change in evapotranspiration during the winter in relation to percent tree mortality. (C) The relationship between understory percent vegetation cover and the percent tree mortality. (D) The relationship between the understory percent vegetation cover and the number of living trees per hectare.

mortality. Although differences in outbreak severity do not appear to explain differences in findings between this and prior studies, other potential explanations could include inherent differences in evapotranspiration patterns due to differences in study area extent, differences in methodology and/or differences in the years used and corresponding interannual variation in precipitation and evaporative demand. The Bright et al. (2013) study area overlapped with ours, for example, but found summer evapotranspiration in un-attacked lodgepole pine forests averaged 1.6 mm day^{-1}. In contrast, we found evapotranspiration in similar forests to be 1.45 ± 0.09 mm day^{-1} in 2011 and 1.32 ± 0.09 mm day^{-1} in 2012. It is possible that our finding of a smaller change to evapotranspiration following outbreak, relative to these previous studies was due, in part, to interannual variation in evaporative demand.

Drier conditions can potentially reduce differences in total evapotranspiration between healthy and recently disturbance stands. A snowmelt driven hydrological cycle, as found in the Rocky Mountains, causes lodgepole pine trees to rely heavily on snowmelt water throughout the growing season (Hu et al., 2010). As summer progresses, water limitations (Knight et al., 1985; Fahey and Knight, 1986) result in an increase to leaf resistance (Chapin et al., 1987) and a decrease in soil moisture (Pataki et al., 2000) in healthy lodgepole pine stands. Soil moisture is elevated in attacked stands, meanwhile, because the reduction in leaf area results in a significant decline in both tree transpiration (Morehouse et al., 2008; Clow et al., 2011) and precipitation interception (Zhang et al., 2004; Pugh and Small, 2012). Elevated soil moisture, as well as enhanced radiative energy inputs and elevated turbulence can increase soil evaporation in attacked stands (Gustafson et al., 2010; Royer et al., 2011), reducing the difference in evapotranspiration between attacked and non-attacked stands in drier years. Similarly, Simonin et al. (2007) found that thinning a semi-arid ponderosa pine stand reduced evapotranspiration during a wet spring when tree stomatal conductance was high, but increased both evaporation and evapotranspiration during a dry summer due to low tree stomatal conductance and therefore limited transpiration in the un-thinned stand. It is also likely that post-attack vegetation dynamics will influence the post-disturbance patterns in evapotranspiration. In contrast to other studies, Brown et al. (2014) measured evapotranspiration using the eddy covariance technique for several years following two severe mountain pine beetle outbreaks and found little change to evapotranspiration. This lack of change was largely attributed to the increased rates of growth in understory and remaining vegetation compensating for the loss of overstory vegetation.

By extending the analysis of post-outbreak patterns in evapotranspiration to 60 years, we found a significant increase in evapotranspiration, relative to non-attacked stands in intermediate aged stands. We attribute this to LAI and fPAR, resulting in peak rates of transpiration in intermediate aged stands. Peaks in winter LAI and fPAR at 30 to 40 years post-outbreak (Fig. 6) suggest that this peak in vegetation is due to a high density of trees, not understory vegetation, which is typically masked by snow during the winter months. Others have found similar patterns with LAI or phytomass. Shiklomanov and Krestovsky (1988), for instance, in a meta-analysis also found phytomass, as well as evapotranspiration, to peak in intermediate aged pine stands (40 years post-harvest). Others have also found LAI to peak in intermediate aged lodgepole pine stands and decline in older stands (Long and Smith, 1992; Vose et al., 1994; Kashian et al., 2005). Similarly, in both lodgepole pine and coniferous forests in general, net primary productivity has been found to peak in intermediate aged stands, specifically between 35 and 55 years in age (Gower et al., 1996; Coursolle et al., 2012).

Performing a seasonally specific sensitivity analysis of the modeled data improved our understanding of the post-outbreak patterns in evapotranspiration. The post-outbreak changes in MODIS evapotranspiration appear to be driven primarily by fPAR, which influences the fraction of plant transpiration versus soil

evaporation in the algorithm, and secondarily by LAI, which influences the rate of plant transpiration and evaporation from the canopy. In addition, seasonal patterns in incoming solar radiation amplify the effect of subtle changes to fPAR and LAI during the growing season. A negative correlation between vegetation amount and the rate of evapotranspiration during winter months was driven by cold temperatures which reduced the rate of transpiration, and a decrease in fPAR which increased the role of evaporation. The accuracy of this evaporation component to capture the rate of snow sublimation and evaporation from melting snow, however, is unknown and is an area in need of improvement within the MODIS evapotranspiration product. In addition to the models' response to temporal and seasonal variation in meteorological parameters, we might expect that outbreaks will result in changes to microclimate, which could affect the rate of evapotranspiration. With fine-scale data, and calculating the change in evapotranspiration relative to local non-attacked forest, it should be possible to separate regional variations in climate due to topography from local variations in microclimate due to an outbreak event. However, the MODIS evapotranspiration product utilizes coarse resolution climate data ($1.00^\circ \times 1.25^\circ$) which limited the ability of the product to respond to fine-scale variation within a biome type. Therefore regardless of the evapotranspiration model's sensitivity to temporal variation in parameters such as relative humidity and air temperature, given the spatial resolution of the climate data relative to the spatial resolution of the outbreak dynamics, using the MODIS evapotranspiration product, patterns in evapotranspiration with time since outbreak are unlikely to be due to changes in microclimate resulting from tree mortality and stand development.

Finally we must recognize errors intrinsic to the indirect estimation of evapotranspiration based on moderate resolution remote sensing. Errors can arise from the algorithm inputs, for instance errors intrinsic to input datasets (fPAR, LAI, albedo) or from the coarseness of the spatial scale (1 km) and interpolated meteorological inputs. Error can also arise from assumptions and structural equations employed by the evapotranspiration algorithm. For instance, because the algorithm does not specifically account for the presence or absence of snow cover, the rate of winter evapotranspiration may show higher rates of intrinsic error, relative to rates calculated for snow-free periods. A more full discussion of the algorithm uncertainties is described in Mu et al. (2011). Additionally, the MODIS evapotranspiration algorithm relies on biome-specific values so that disturbance driven changes to vegetation type and species within a given biome can introduce additional uncertainty. We have taken methodological steps to remove confounding effects on our analysis of the changes in evapotranspiration post beetle outbreak. Calculating change in evapotranspiration as a change from local non-attacked forest has improved our confidence in the directionality of changes over the observed time intervals. Additionally, our sub-selection of MODIS evapotranspiration dates was necessary in order to match the timing of our field data collection to the timing of the satellite data collection. This coordination of dates improved our confidence regarding the signal during each attack stage. Despite our finding of ecologically consistent patterns in the response of evapotranspiration with years since outbreak, it is important to note that although the directionality of patterns with time since outbreak were consistent within the study, the magnitude of that change, whether compared across a landscape or relative to local non-attacked forests is subject to greater uncertainty.

5. Conclusions

The MODIS evapotranspiration product produced ecologically realistic results when applied at a regional scale to quantify within biome variation following mountain pine beetle attack and tree mortality events. During the growing season, mountain pine beetle outbreaks initially resulted in a significant reduction in evapotranspiration as a consequence of a decrease in fPAR and LAI. However, intermediate-aged stands experienced an approximately equivalent increase in evapotranspiration corresponding with peaks in lodgepole pine stand density and stand LAI and fPAR. High incoming solar radiation during the summer months amplified changes to evapotranspiration even with relatively minor changes to summer fPAR and LAI owing to rapid regeneration of understory vegetation. Although the regeneration of understory vegetation was positively correlated with outbreak severity, change to evapotranspiration still increased with outbreak severity during the summer season suggesting that transpiration from understory vegetation did not fully compensate for tree mortality. In conclusion, a focus on the initial post-outbreak reduction in growing season evapotranspiration, as documented by previous studies, misses potentially opposing modifications in evapotranspiration experienced within different seasons as well as by intermediate-aged stands, when stand density and leaf area peaks. Mountain pine beetle outbreaks cause sizeable changes in stand structure and evapotranspiration with long-lasting impacts that could affect water resource dynamics across western North America.

Acknowledgements

This work was supported by NASA Headquarters under the NASA Earth and Space Science Fellowship Program (Grant no. 12-Earth12R-59 and 13-Earth13R-8). Additional financial support was received from the NASA ROSES09 Science of Terra and Aqua program (Grant no. NNX11AG53G) as well as the National Science Foundation (Grant no. 1262691). We thank Rocky Mountain National Park for their field support and Marcus Pasay for his assistance with field work. We also thank Dominik Kulakowski and Dan Jarvis for providing the dendroecological plot data, Brian Howell and Justin Backsen of the USFS Region 2, for their assistance with the historical ADS surveys, and the anonymous reviewers for the valuable comments.

Appendix A. Appendix

In the analysis, change in evapotranspiration with years since outbreak start was calculated as percent change to help normalize our calculation of change from local non-attacked forest. However, we can also calculate evapotranspiration as absolute change in evapotranspiration (mm day^{-1}) (Fig. A1). We found similar seasonal patterns of change regardless of whether evapotranspiration was calculated as absolute or percent change.

To better understand the potential validity or flaws in utilizing the MODIS evapotranspiration algorithm in the winter months, we used the modeled data to explore how the model inputs were influencing the calculated sub-components of evapotranspiration (soil evaporation, transpiration and wet canopy evaporation). This was necessary because snow sublimation is not explicitly modeled in the current MODIS evapotranspiration algorithm. In particular we wanted to understand the negative correlation between winter evapotranspiration and vegetation amount. We hope this analysis is helpful in improving future versions of the MODIS evapotranspiration product. Importantly, we found that regardless of stand structure or years since outbreak, the distribution of modeled evapotranspiration between plant transpiration and soil evaporation was strongly seasonally dependent. For instance, within non-attacked plots, growing season evapotranspiration was dominated by transpiration (0.9 ± 0.03 mm day^{-1}) relative to soil evaporation (0.05 ± 0.005 mm day^{-1}) (Fig. 7). In contrast, winter

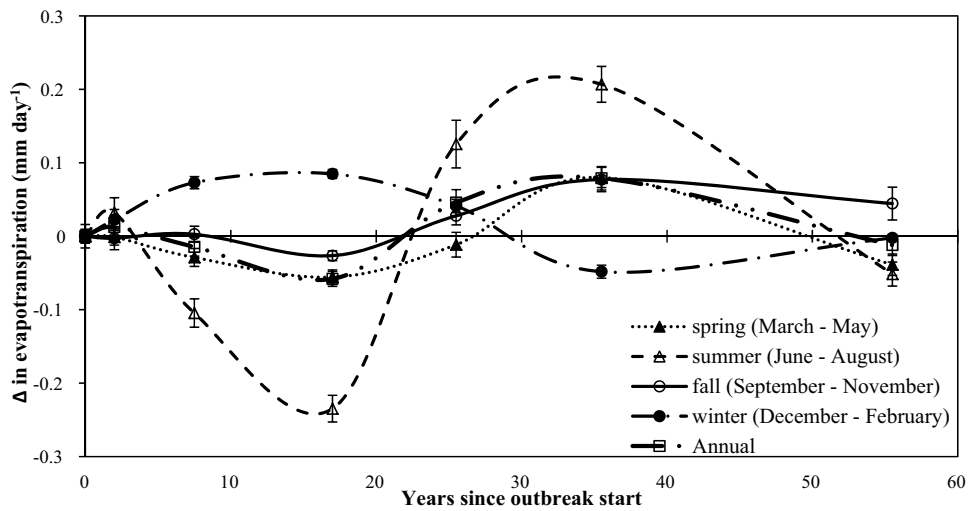

Fig. A1. Absolute change in seasonal and annual evapotranspiration with years since outbreak start. Change is calculated relative to local, for each plot, non-attacked forest. Error bars are plus and minus standard error.

evapotranspiration within non-attacked plots was dominated by soil evaporation (or snow sublimation) (0.5 ± 0.02 mm day^{-1}), relative to transpiration (0.04 ± 0.005 mm day^{-1}) (Fig. 7). The dependence of the distribution of evapotranspiration components on season is even clearer if we artificially manipulate the fraction vegetation cover versus bare soil. Across all plots during the growing season, if we assume complete vegetation cover, the rate of evapotranspiration exceeds that if we assume complete bare soil (1.7 ± 0.03 mm day^{-1} compared to 0.2 ± 0.01 mm day^{-1}, respectively). The opposite is observed during the winter months, where assuming complete vegetation cover leads to a lower rate of evapotranspiration than if we assume complete bare soil (or snow) (0.05 ± 0.004 mm day^{-1} compared to 0.9 ± 0.01 mm day^{-1}, respectively) (Fig. A2). Therefore, across attacked plots, the winter reduction in transpiration was the consequence of low air temperatures which resulted in partial to complete stomatal closure (as defined by the biome specific temperature driven thresholds in the model's algorithm) as well as significantly lower LAI (0.62 ± 0.02 plants m^2 ground m^{-2} in winter compared to 1.41 ± 0.02 plants m^2 ground m^{-2} in the growing season ($p < 0.01$)) and fPAR values (0.41 ± 0.01 in winter compared to 0.54 ± 0.004 in the growing season ($p < 0.01$)). The winter increase in the rate of soil evaporation or snow sublimation was a consequence of both a lower fPAR, which increased the fraction bare ground from which soil evaporation or snow sublimation was calculated on, as well as significantly higher rates of relative humidity during the winter (0.56 ± 0.01 in winter compared to 0.39 ± 0.004 in the growing season ($p < 0.01$), which is used as a scalar to translate potential evaporation to actual evaporation (or sublimation), and increases the amount of evaporation (or sublimation) from wet canopies. Because the evapotranspiration model in winter was sensitive to changes in fPAR and the rate of soil evaporation (or snow sublimation) exceeded transpiration, a decrease in fPAR increased the bare ground component, and therefore the total rate of evapotranspiration. In turn, because plant transpiration dominated evapotranspiration during the summer months, the rate of summer evapotranspiration correlated positively with vegetation amount following an outbreak.

In addition to investigating the dynamics of the MODIS evapotranspiration product sub-components, exploring the directional relationships between the MODIS evapotranspiration product climate input parameters (relative humidity, vapor pressure, incoming solar radiation, temperature, and atmospheric pressure) and seasonal patterns in evapotranspiration can help validate the product's application to address ecological questions at a regional scale and to quantify within biome variation. The model, for instance, was found to be sensitive to relative humidity and vapor pressure during both the growing season and winter

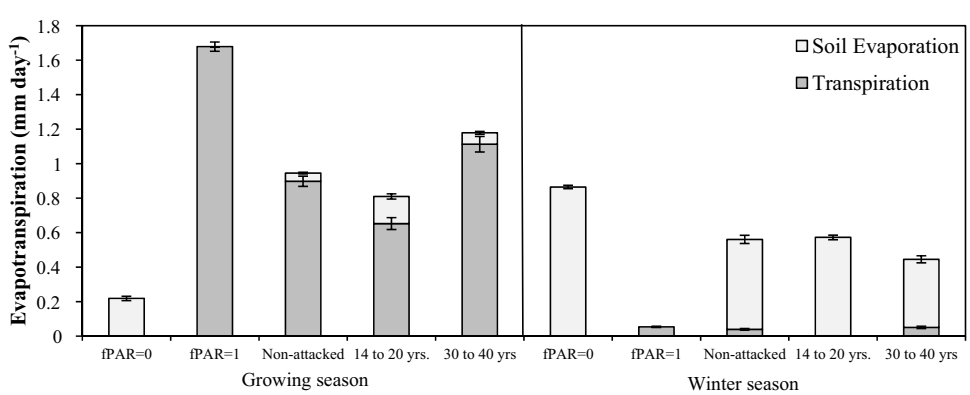

Fig. A2. Seasonal rates of soil evaporation (and snow sublimation) versus transpiration are shown for comparison purposes for bare ground pixels (fPAR = 0), pixels with complete vegetation cover (fPAR = 1), and pixels for key intervals with time since outbreak. It is important to note that evapotranspiration should not be directly compared between non-attacked, 14 to 20 year, and 30 to 40 year classes given the climate variations that exist between these data populations. Seasonal differences and the partitioning between soil evaporation and transpiration are, however, robust to this variation. Error bars show plus and minus standard error.

months (Fig. 5). In the evapotranspiration algorithm, vapor pressure influences vapor pressure deficit, which is directly used in the calculation of transpiration, soil evaporation (and snow sublimation) and wet canopy evaporation, as well as surface conductance. Relative humidity is used to scale the rate of soil evaporation and if >70%, then to determine the fraction of wet canopy evaporation (Mu et al., 2011). In both the growing season and winter season, increases in relative humidity and vapor pressure increased the rate of bare ground evaporation and decreased the rate of plant transpiration. Additionally, in both seasons, the decrease in plant transpiration was exceeded by the increase in bare ground evaporation, meaning increases in relative humidity and vapor pressure increased evapotranspiration in both seasons. As would be expected, evapotranspiration increased with increasing temperature and incoming solar radiation during both the growing season and winter months (Fig. 5). Incoming shortwave radiation informs net radiation or available energy, while temperature is directly used in many of the algorithm calculations including to quantify net radiation, soil heat flux, air density, the slope of the curve relating saturated water vapor pressure to temperature, and finally several resistance parameters including the total aerodynamic resistance to vapor transport, the radiative heat transport and to limit stomatal conductance (Mu et al., 2011). Finally, evapotranspiration showed opposite changes with increasing elevation in the growing season versus winter season (Fig. 5). Elevation drives the calculation of atmospheric pressure, which is then used to calculate the psychrometric constant, air density and surface conductance (Mu et al., 2011). In both the winter and growing season, an increase in elevation (or atmospheric pressure) increased soil evaporation by decreasing air density and in turn, increasing aerodynamic conductance, and decreased transpiration by decreasing air pressure and in turn, decreasing surface conductance. In winter, the change to soil evaporation (or snow sublimation) dominated, meaning an increase in elevation (or atmospheric pressure) increased evapotranspiration, while in the growing season, the change to transpiration dominated, meaning an increase in elevation (or atmospheric pressure) decreased evapotranspiration.

References

Adams, H.D., Luce, C.H., Breshears, D.D., et al., 2012. Ecohydrological consequences of drought- and infestation-triggered tree die-off: insights and hypotheses. Ecohydrology 5 (2), 145–159.

Alfaro, R.I., Campbell, E., Hawkes, B.C., 2010. Historical frequency, intensity and extent of mountain pine beetle disturbance in British Columbia. In: Mountain Pine Beetle Working Paper 2009–30. Natural Resources Canada, Canadian Forest Service, Pacific Forestry Centre, Victoria, BC.

Allen, R.G., Tasumi, M., Morse, A., Trezza, R., 2005. A Landsat-based energy balance and evapotranspiration model in Western US water rights regulation and planning. Irrig. Drain. Syst. 19, 251–268.

Amman, G.D., 1977. The role of the mountain pine beetle in lodgepole pine ecosystems: impact on succession. In: Mattson, W.J. (Ed.), Proceedings in Life Sciences: The Role of Arthropods in Forest Ecosystems. Springer-Verlag, New York, NY, pp. 3–18.

Amiro, B.D., Barr, A.G., Black, T.A., et al., 2006. Carbon, energy and water fluxes at mature and disturbed forest sites, Saskatchewan, Canada. Agric. For. Meteorol. 136, 237–251.

Axelson, J.N., Alfaro, R.I., Hawkes, B.C., 2009. Influence of fire and mountain pine beetle on the dynamics of lodgepole pine stands in British Columbia, Canada. For. Ecol. Manage. 257, 1874–1882.

Bala, G., Caldeira, K., Wickett, M., Phillips, T.J., Lobell, D.B., Mirin, A., 2007. Combined climate and carbon-cycle effects of large-scale deforestation. Proc. Natl. Acad. Sci. 104 (16), 6550–6555.

Barker, C., Amiro, B.D., Kwon, H., Ewers, B.E., Angstmann, J., 2009. Evapotranspiration in intermediate-aged and mature fens and upland black spruce boreal forests. Ecohydrology 2, 462–471.

Bastiaanssen, W.G.M., Menenti, M., Feddes, R.A., Holtslag, A.A.M., 1998. A remote sensing surface energy balance algorithm for land (SEBAL). J. Hydrol. 212–213, 198–212.

Berg, E.E., Henry, J.D., Fastie, C.I., de Volder, A.D., Matsuoka, S.M., 2006. Spruce beetle outbreaks on the Kenai Peninsula, Alaska and Kluane National Park and Reserve, Yukon Territory: relationship to summer temperatures and regional differences in disturbance regimes. For. Ecol. Manage. 227, 219–232.

Bethlahmy, N., 1974. More streamflow after a bark beetle epidemic. J. Hydrol. 23, 185–189.

Bewley, D., Alila, Y., Varhola, A., 2010. Variability of snow water equivalent and snow energetic across a large catchment subject to Mountain Pine Beetle infestation and rapid salvage logging. J. Hydrol. 388, 464–479.

Bonan, G., 2008. Ecological Climatology: Concepts and Applications, second ed. Cambridge University Press, Cambridge, MA, pp. 550.

Boon, S., 2012. Snow accumulation following forest disturbance. Ecohydrology 5 (3), 279–285.

Bosch, J.M., Hewlett, J.D., 1982. A review of catchment studies to determine the effect of vegetative changes on water yield and evapotranspiration. J. Hydrol. 55, 3–23.

Bright, B.C., Hicke, J.A., Meddens, A.J.H., 2013. Effects of bark beetle-caused tree mortality on biogeochemical and biogeophysical MODIS products. J. Geophys. Res. Biogeosci. 118, 974–982.

Brown, M.G., Black, T.A., Nesic, Z., Foord, V.N., Spittlehouse, D.L., Fredeen, A.L., Grant, N.J., Burton, P.J., Trofymow, J.A., 2010. Impact of mountain pine beetle on the net ecosystem production of lodgepole pine stands in British Columbia. Agric. For. Meteorol. 150, 254–264.

Brown, M.G., Black, T.A., Nesic, Z., Foord, V.N., Spittlehouse, D.L., Fredeen, A.L., Bowler, R., Grant, N.J., Burton, P.J., Trofymow, J.A., Lessard, D., Meyer, G., 2014. Evapotranspiration and canopy characteristics of two Lodgepole pine stands following mountain pine beetle attack. Hydrol. Processes 28, 3326–3340.

Chapin III, F.S., Bloom, A.J., Field, C.B., Waring, R.H., 1987. Plant responses to multiple environmental factors. BioScience 37 (1), 49–57.

Clark, K.L., Skowronski, N., Gallagher, M., Renninger, H., Schäfer, K., 2012. Effects of invasive insects and fire on forest energy exchange and evapotranspiration in the New Jersey pinelands. Agric. For. Meteorol. 166–167, 50–61.

Cleugh, H.A., Leuning, R., Mu, Q., Running, S.W., 2007. Regional evaporation estimates from flux tower and MODIS satellite data. Remote Sens. Environ. 106, 285–304.

Clow, D.W., Rhoades, C., Briggs, J., Caldwell, M., Lewis, W.M.J., 2011. Responses of soil and water chemistry to mountain pine beetle induced tree mortality in Grand County, Colorado. Appl. Geochem. 26, S174–S178.

Constantin, J., Grelle, A., Ibrom, A., Morgenstern, K., 1999. Flux partitioning between understorey and overstorey in a boreal spruce/pine forest determined by the eddy covariance method. Agric. For. Meteorol. 98–99, 629–643.

Coursolle, C., Margolis, H.A., Giasson, M.A., et al., 2012. Influence of stand age on the magnitude and seasonality of carbon fluxes in Canadian forests. Agric. For. Meteorol. 165, 136–148.

Eidenshink, J., Schwind, B., Brewer, K., Zhu, Z., Quayle, B., Howard, S., 2007. A project for monitoring tends in burn severity. Fire Ecol. 3 (1), 3–21.

Fahey, T.J., Knight, D.H., 1986. Lodgepole pine ecosystems: biotic processes play a critical role in regulating material flux in Rocky Mountain lodgepole pine forests. BioScience 36 (9), 610–617.

Farley, K.A., Jobbagy, E.G., Jackson, R.B., 2005. Effects of afforestation on water yield: a global synthesis with implications for policy. Global Change Biol. 11, 1565–1576.

Friedl, M.A., McIver, D.K., Hodges, J.C.F., Zhang, X.Y., Muchoney, D., Strahler, A.H., Woodcock, C.E., Gopal, S., Schneider, A., Cooper, A., Baccini, A., Gao, F., Schaaf, C., 2002. Global land cover mapping from MODIS: algorithms and early results. Remote Sens. Environ. 83, 287–302.

Gholz, H.L., Clark, K.L., 2002. Energy exchange across a chronosequence of slash pine forests in Florida. Agric. For. Meteorol. 112, 87–102.

Gower, S.T., McMurtrie, R.E., Murty, D., 1996. Aboveground net primary production decline with stand age: potential causes. Tree 11 (9), 378–382.

Griesbauer, H., Green, S., 2006. Examining the utility of advance regeneration for reforestation and timber production in unsalvaged stands killed by the mountain pine beetle: controlling factors and management implications. B.C. J. Ecosyst. Manage. 7 (2), 81–92.

Gustafson, J.R., Brooks, P.D., Molotch, N.P., Veatch, W., 2010. Quantifying snow sublimation using natural tracer concentrations and isotopic fractionation in a forested catchment. Water Resour. Res. 46, W12511, http://dx.doi.org/10.1029/2009WR009060.

Heath, R., Alfaro, R.I., 1990. Growth response in a Douglas-fir/lodgepole pine stand after thinning of lodgepole pine by the mountain pine beetle: a case study. J. Entomol. Soc. B.C. 87, 16–21.

Hu, J., Moore, D.J.P., Burns, S.P., Monson, R.K., 2010. Longer growing seasons lead to less carbon sequestration by a subalpine forest. Global Change Biol. 16 (20), 771–783.

Jassal, R.S., Black, T.A., Spittlehouse, D.L., Brömmer, C., Nesic, Z., 2009. Evapotranspiration and water use efficiency in different-aged Pacific Northwest Douglas-fir stands. Agric. For. Meteorol. 149, 1168–1178.

Jin, Y., Schaaf, C.B., Gao, F., Li, X., Strahler, A.H., Lucht, W., Liang, S., 2003. Consistency of MODIS surface BRDF/Albedo retrieval. 1. Algorithm performance. J. Geophys. Res. 108 (D5), 4158, http://dx.doi.org/10.1029/2002JD002803.

Jones, J.A., Post, D.A., 2004. Seasonal and successional streamflow response to forest cutting and regrowth in the northwest and eastern United States. Water Resour. Res. 40, W05203, http://dx.doi.org/10.1029/2003WR002952.

Kashian, D.M., Turner, M.G., Romme, W.H., 2005. Variability in leaf area and stemwood increment along a 300-year lodgepole pine chronosequence. Ecosystems 8, 48–61.

Klutsch, J.G., Negron, J.F., Costello, S.L., Rhoades, C.C., West, D.R., Popp, R., Caissie, R., 2009. Characteristics and downed woody debris accumulations associated with mountain pine beetle (*Dendroctonus ponderosae* Hopkins) outbreak in Colorado. For. Ecol. Manage. 258, 641–649.

Knight, D.H., Fahey, T.J., Running, S.W., 1985. Water and nutrient outflow from contrasting lodgepole pine forests in Wyoming. Ecol. Monogr. 55, 29–48.
Kulakowski, D., Jarvis, D., 2011. The influence of mountain pine beetle outbreaks on severe wildfires in northwestern Colorado and southern Wyoming: a look at the past century. For. Ecol. Manage. 261, 1686–1696.
Kulakowski, D., Jarvis, D., Veblen, T.T., Smith, J., 2012. Stand-replacing fires reduce susceptibility of lodgepole pine to mountain pine beetle outbreaks in Colorado. J. Biogeogr. 39, 2052–2060.
Kummerow, C., Barnes, W., Kozu, T., Shiue, J., Simpson, J., 1998. The tropical rainfall measuring mission (TRMM) sensor package. J. Atmos. Oceanic Technol. 15, 809–817.
Kustas, W.P., Norman, J.M., 1999. Evaluation of soil and vegetation heat flux predictions using a simple two-source model with radiometric temperatures for partial canopy cover. Agric. For. Meteorol. 94, 13–29.
Likens, G.E., Driscoll, C.T., Buso, D.C., et al., 1994. The biogeochemistry of potassium at Hubbard Brook. Biogeochemistry 25, 61–125.
Long, J.N., Smith, F.W., 1992. Volume increment in *Pinus contorta* var. *latifolia*: the influence of stand development and crown dynamics. For. Ecol. Manage. 53, 53–64.
Maness, H., Kushner, P.J., Fung, I., 2012. Summertime climate response to mountain pine beetle disturbance in British Columbia. Nat. Geosci. 6, 65–70.
McCarthy, J., 2001. Gap dynamics of forest trees: a review with particular attention to boreal forests. Environ. Rev.V 9, 1–59.
Messier, C., Doucet, R., Ruel, J., Claveau, Y., Kelly, C., Lechowicz, M.J., 1999. Functional ecology of advance regeneration in relation to light in boreal forests. Can. J. For. Res. 29, 812–823.
Mikkelson, K.M., Maxwell, R.M., Ferguson, I., Stednick, J.D., McCray, J.E., Sharp, J.O., 2013. Mountain pine beetle infestation impacts: modeling water and energy budgets at the hill-slope scale. Ecohydrology 6 (1), 64–72.
Mitchell, R.G., Preisler, H.K., 1998. Fall rate of lodgepole pine killed by the mountain pine beetle in central Oregon. West. J. Appl. For. 13 (1), 23–26.
Moore, G.W., Bond, B.J., Jones, J.A., Phillips, N., Meinzer, F.C., 2004. Structural and compositional controls on transpiration in 49- and 450-year-old riparian forests in western Oregon, USA. Tree Physiol. 24, 481–491.
Monteith, J.L., 1965. Evaporation and environment. In: Fogg, G.E. (Ed.), Symposium of the Society for Experimental Biology, The State and Movement of Water in Living Organisms. Academic Press, Inc, New York, NY, pp. 205–234.
Morehouse, K., Johns, T., Kaye, J., Kaye, M., 2008. Carbon and nitrogen cycling immediately following bark beetle outbreaks in southwestern ponderosa pine forests. For. Ecol. Manage. 255, 2698–2708.
Mu, Q., Heinsch, F.A., Zhao, M., Running, S.W., 2007. Development of a global evapotranspiration algorithm based on MODIS and global meteorology. Remote Sens. Environ. 111, 519–536.
Mu, Q., Zhao, M., Running, S.W., 2011. Improvements to a MODIS global terrestrial evapotranspiration algorithm. Remote Sens. Environ. 115, 1781–1800.
Musselman, K., Molotch, N.P., Brooks, P.D., 2008. Quantifying the effects of forest vegetation on snow accumulation, ablation and potential meltwater inputs, Valles Caldera National Preserve, NM, USA. Hydrol. Processes 22, 2767–2776.
Myneni, R.B., Hoffman, S., Knyazikhin, Y., 2002. Global products of vegetation leaf area and fraction absorbed PAR from year one of MODIS data. Remote Sens. Environ. 83, 214–231.
Naranjo, J.A.B., Stahl, K., Weiler, M., 2012. Evapotranspiration and land cover transitions: long-term watershed response in recovering forested ecosystems. Ecohydrology 5, 721–732.
Nishida, K., Nemani, R.R., Running, S.W., Glassy, J.M., 2003. Development of an evapotranspiration index from Aqua/MODIS for monitoring surface moisture status. IEEE Trans. 41, 1–9.
Pataki, D.E., Oren, R., Smith, W.K., 2000. Sap flux of co-occurring species in a western subalpine forest during seasonal soil drought. Ecology 81 (9), 2557–2566.
Potts, D.F., 1984. Hydrologic impacts of a large scale mountain pine beetle (*Dendroctonus ponderosae* Hopkins) epidemic. In: Water Resources Bulletin Paper No. 83122., pp. 373–377.
Pugh, E., Small, E., 2012. The impact of pine beetle infestation on snow accumulation and melt in the headwaters of the Colorado River. Ecohydrology 5 (4), 467–477.
Raffa, K.F., Aukema, B.H., Bentz, B.J., Carroll, A.L., Hicke, J.A., Turner, M.G., Romme, W.H., 2008. Cross-scale drivers of natural disturbances prone to anthropogenic amplification: the dynamics of bark beetle eruptions. BioScience 58, 501–517.
Roe, A., Amman, G., 1970. Mountain pine beetle in lodgepole pine forests. In: Research Paper INT-71. USDA Forest Service, Intermountain Research Station, pp. 26.
Royer, P.D., Cobb, N.S., Clifford, M.J., Huang, C.Y., Breshears, D.D., Adams, H.D., Villegas, J.C., 2011. Extreme climatic event-triggered overstory vegetation loss increases understory solar input regionally: primary and secondary ecological implications. J. Ecol. 99 (3), 714–723.
Schaaf, C.B., Gao, F., Strahler, A.H., et al., 2002. First operational BRDF, albedo nadir reflectance products from MODIS. Remote Sens. Environ. 83, 135–148.
Scott, D.F., Smith, R.E., 1997. Preliminary empirical models to predict reductions in annual and low flows resulting from afforestation. Water S.A. 23, 135–140.
Shiklomanov, I.A., Krestovsky, O.I., 1988. The influence of forests and forest reclamation practice on streamflow and water balance. In: Reynolds, E.R.C., Thompson, F.B. (Eds.), Forests, Climate, and Hydrology: Regional Impacts. United Nations University, Tokyo, pp. 78–116.
Simonin, K., Kolb, T.E., Montes-Helu, M., Koch, G.W., 2007. The influence of thinning on components of stand water balance in a ponderosa pine forest stand during and after extreme drought. Agric. For. Meteorol. 143, 266–276.
Swift, L.W., Swank, W.T., 1981. Long-term responses of streamflow following clearcutting and regrowth. Hydrol. Sci. Bull. 26, 245–256.
United States Forest Service (USFS), 2011. Western Bark Beetle Strategy. USDA Forest Service.
Wickman, B.E., Seidel, K.W., Starr, G.L., 1986. Natural regeneration 10 years after a Douglas-fir tussock moth outbreak in northeastern Oregon. In: Research Paper PNWRP. U.S. Department of Agriculture Forest Service, Pacific Northwest Research Station, Portland, Oregon, pp. 370.
Wiedinmyer, C., Barlage, M., Tewari, M., Chen, F., 2012. Meteorological impacts of forest mortality due to insect infestation in Colorado. Earth Interact. 16, 1–11.
Wilson, K.B., Hansonb, P.J., Baldocchi, D.D., 2000. Factors controlling evaporation and energy partitioning beneath a deciduous forest over an annual cycle. Agric. For. Meteorol. 102, 83–103.
Wohlgemuth, T., Kull, P., Wuthrich, H., 2002. Disturbance of microsites and early tree regeneration after windthrow in Swiss mountain forests due to the winter storm Vivian 1990. For. Snow Landscape Res. 77, 17–47.
Vanderhoof, M., Williams, C.A., Shuai, Y., Jarvis, D., Kulakowski, D., Masek, J., 2014. Albedo-induced radiative forcing from mountain pine beetle outbreaks in forests, south-central Rocky Mountains: magnitude, persistence, and relation to outbreak severity. Biogeosciences 11, 563–575.
Vose, J.M., Dougherty, P.M., Long, J.N., Smith, F.W., Gholz, H.L., Curran, P.J., 1994. Factors influencing the amount and distribution of leaf area of pine stands. Ecol. Bull. 43, 102–114.
Zhang, Y.S., Suzuki, K., Kadota, T., Ohata, T., 2004. Sublimation from snow surface in southern mountain taiga of eastern Siberia. J. Geophys. Res. 109, D21103.